

Dynamique des ressauts de marée et mascarets en milieu estuarien

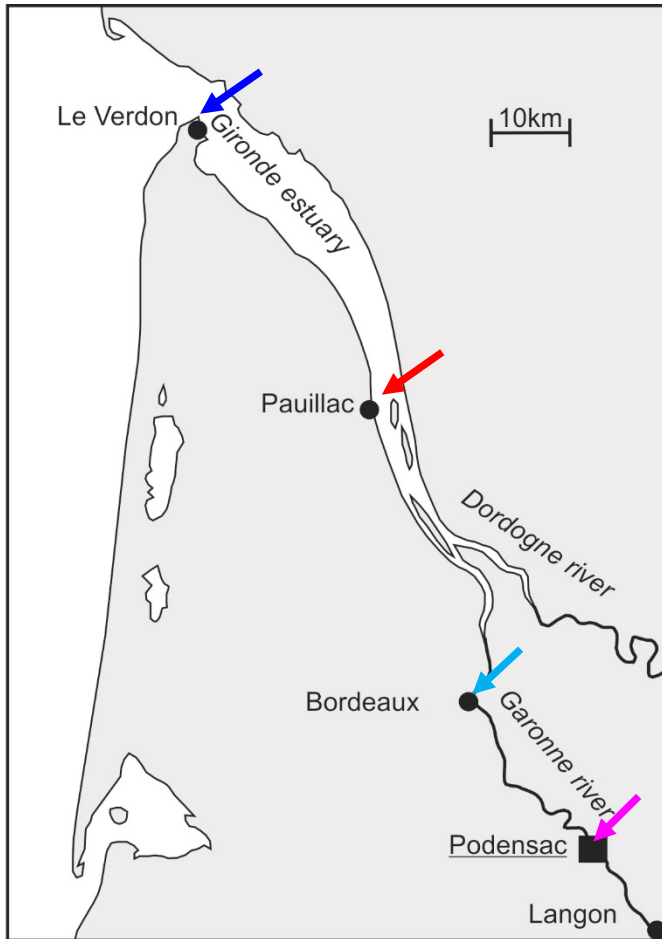


Philippe Bonneton

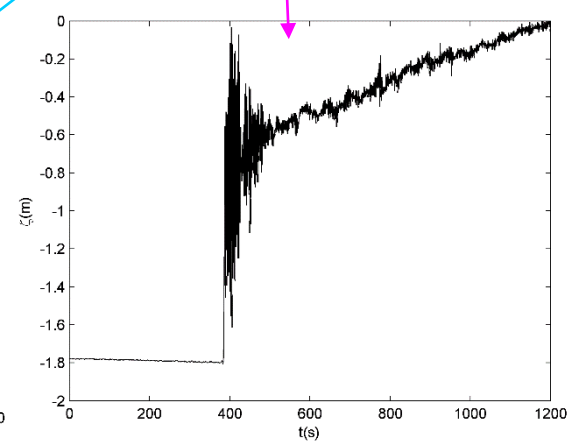
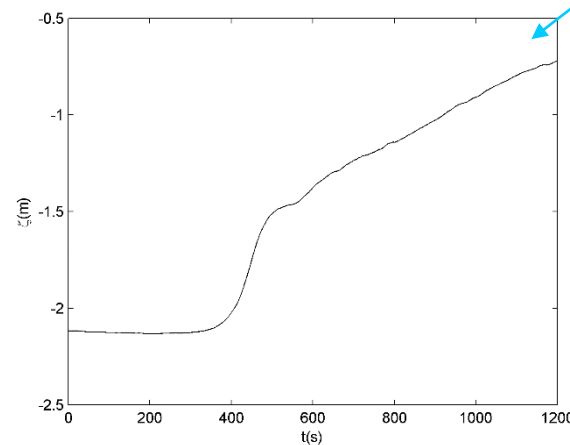
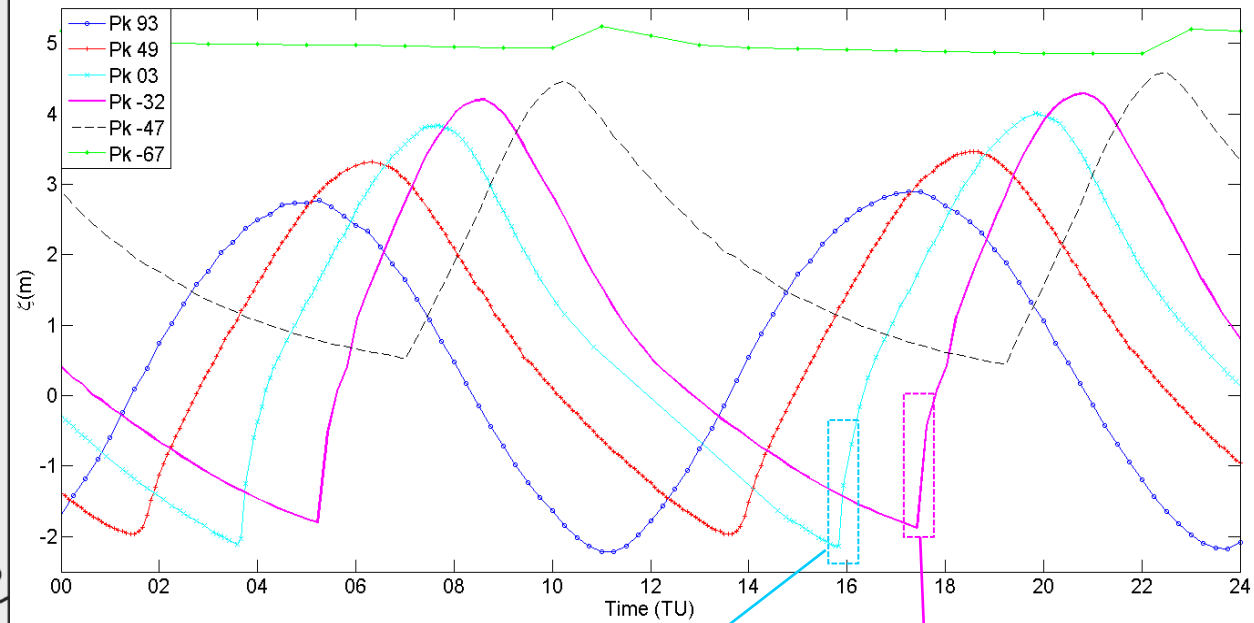
EPOC, METHYS team, Bordeaux Univ., CNRS



Garonne - Bonneton et al., 2015



Large amplitude spring tide

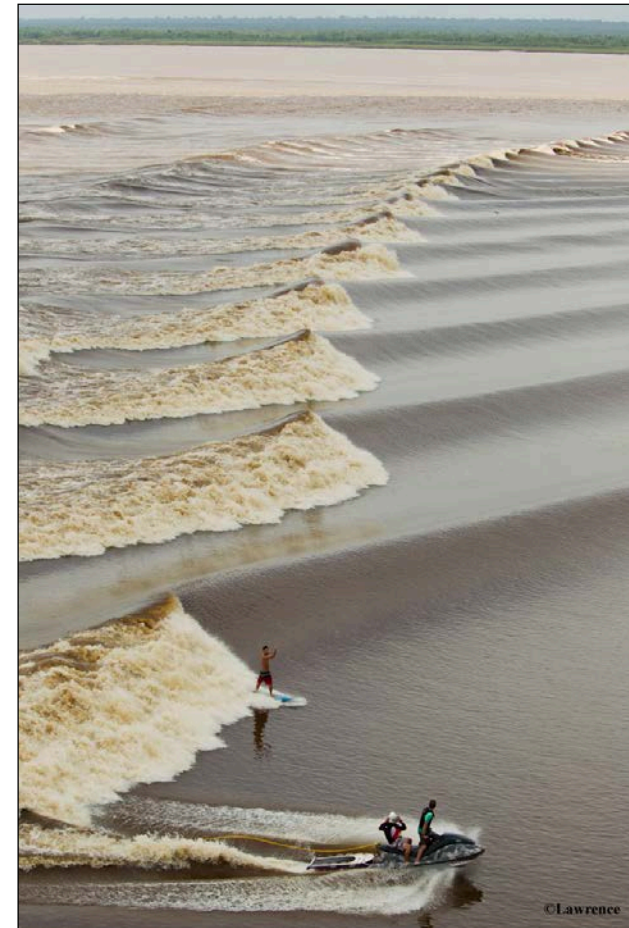




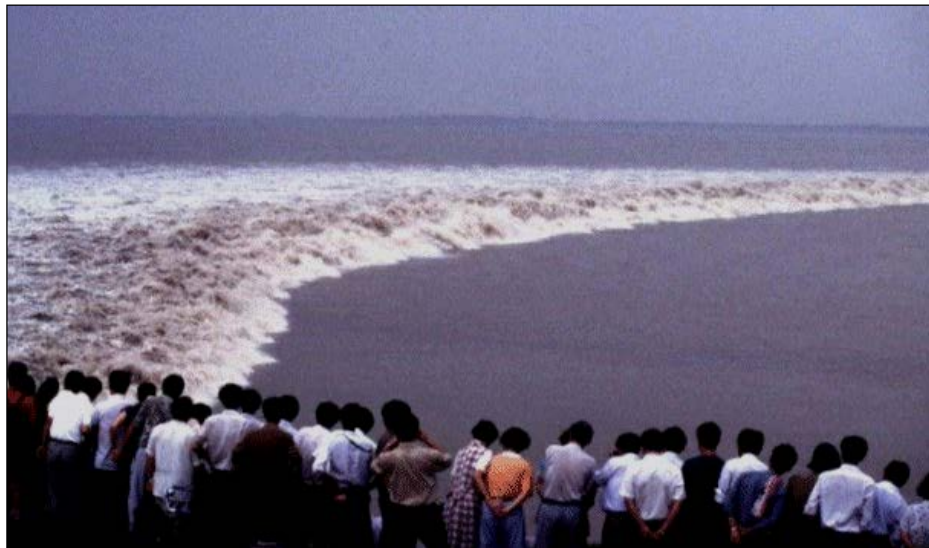
Severn River - England



Amazon River – Brazil (Pororoca)



Kampar River – Sumatra (Bono)



Qiantang River – China

un phénomène intense, mais fragile, qui a disparu dans de nombreux estuaires

Phénomène ondulatoire spectaculaire mal connu

→ observations in situ qualitatives (visuelles)

e.g. Bartsch-Winkler and Lynch 1988, Chanson 2012

Analyse détaillée de la dynamique des ressauts de marée

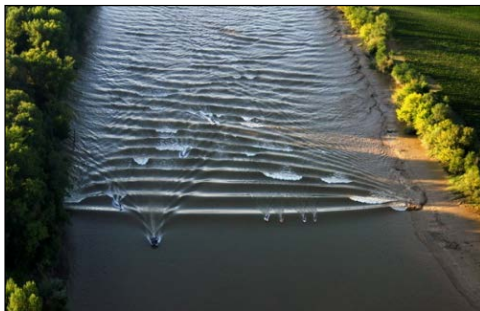
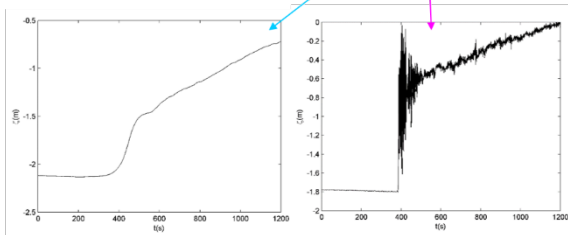
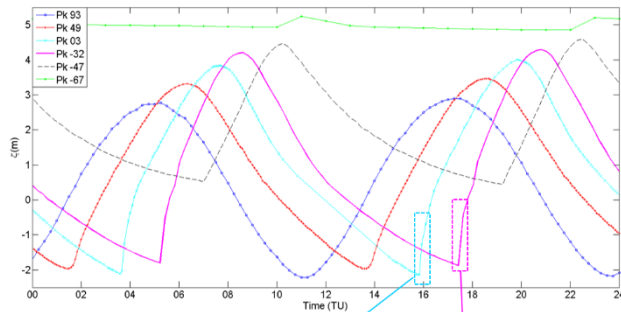
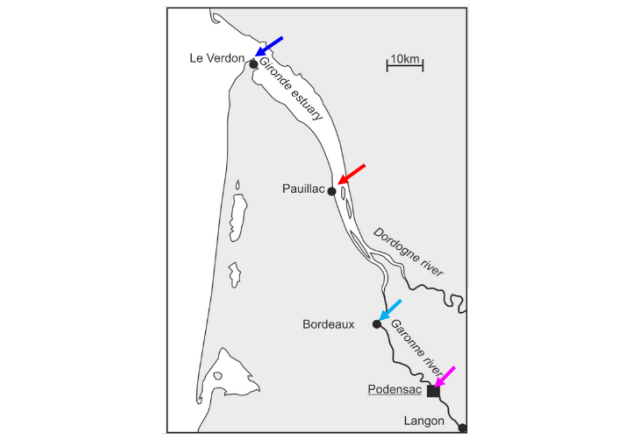
→ campagnes de mesures intensives (Gironde/Garonne et Seine)

→ modélisation numérique (équations de Serre / Green Naghdi)

Grande échelle

Transformation de la marée et
mécanisme de formation des RM

- Bonneton, P., Filippini, A.G., Arpaia, L., Bonneton, N. and Ricchiuto, M. 2016. Conditions for tidal bore formation in convergent alluvial estuaries. *Estuarine, Coastal and Shelf Science*. **172**, 121-127
- Filippini, A.G., Arpaia, L., Bonneton, P., and Ricchiuto, M. 2018. Modeling analysis of tidal bore formation in convergent estuaries. *Eur. J. Mech. B Fluids*.



Petite échelle

Dynamique haute fréquence des RM

- Bonneton, N., Bonneton, P., Parisot, J-P., Sottolichio, A. and Detandt G. 2012. Tidal bore and Mascaret - example of Garonne and Seine Rivers. *Comptes Rendus Geosciences*, **344**, 508-515.
- Bonneton, P., Bonneton, N., Parisot, J-P. and Castelle, B. 2015. Tidal bore dynamics in funnel-shaped estuaries. *J. Geophys. Res.: Ocean*, **120**(2), 923-941.
- Chassagne R., Filippini A., Ricchiuto M. and Bonneton P. 2018. Dispersive-like bores in channels with sloping banks. In preparation

↓
Exposé

❑ field measurements

→ *Bonneton N., Castelle B., Detandt G., Parisot J-P., Sottolichio A. (EPOC, METHYS team, Bordeaux)*

→ *Frappart F., Roussel N., Darrozes J. (OMP, Toulouse)*

→ *Martins K. (Bath University)*

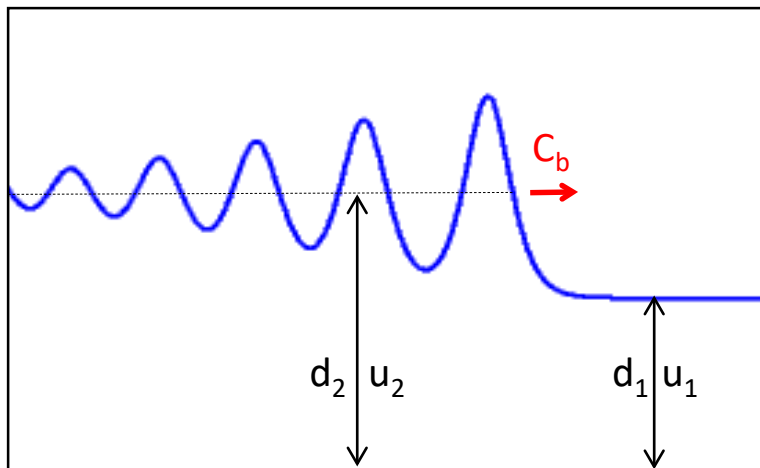
❑ long wave modeling

→ *Ricchuito M., Arpaia L., Filippini A. (INRIA, Bordeaux), Chassagne R. (LEGI)*

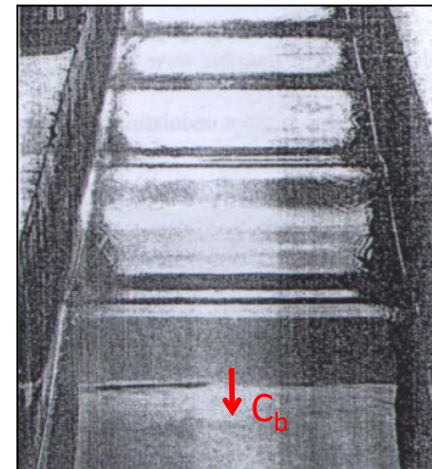
Plan

- I. Introduction
- II. Ondes de Favre
- III. Observations in situ
- IV. Ressaut de marée de faible cambrure
- V. Conclusion and perspectives

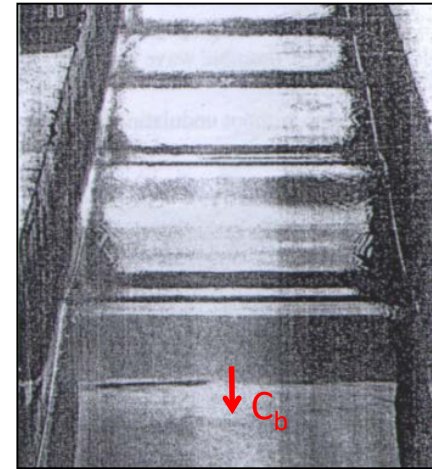
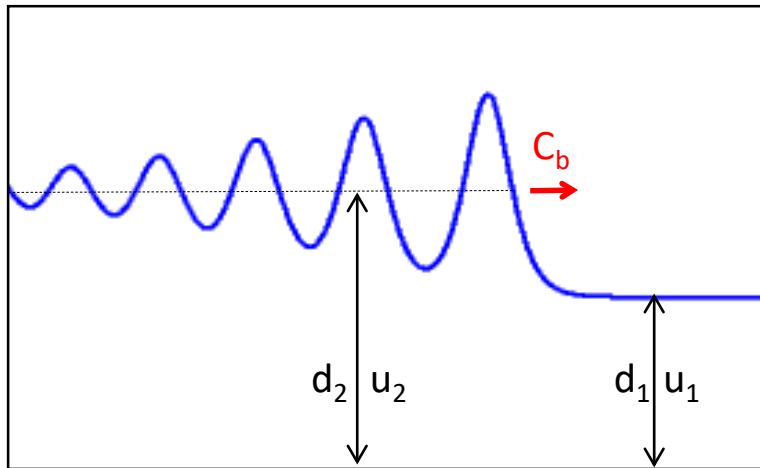
Analogie entre les ressauts de marée ondulants et les ondes de Favre



Ressaut en translation ondulant 2D



Ondes de Favre



Mathematical and physical theories:

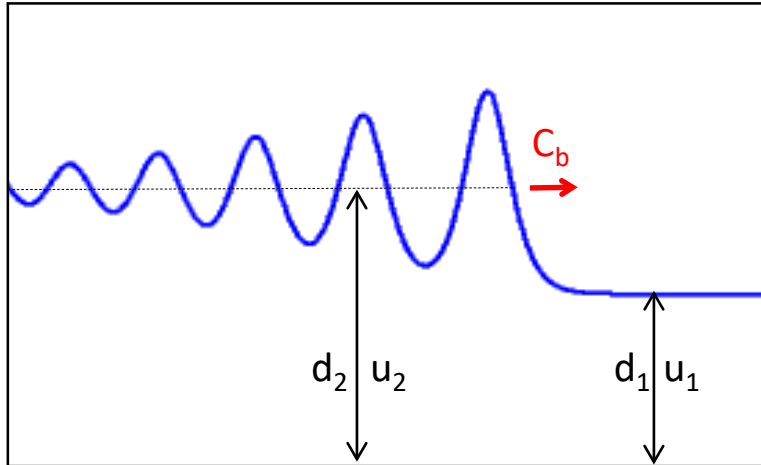
Rayleigh 1914, Lemoine 1948, Serre 1954, Benjamin and Lighthill 1954, Johnson 1970, Gurevich and Pitaevskii 1973, El et al. 2006 and many others ...

Laboratory experiments:

Favre 1935, Sandover and Zienkiewics 1957, Bennet & Cunge 1971, Treske 1994, Chanson 1996 & 2009, Soares Frazao and Zech 2002, Simon 2013, Furgerot 2014, David et al. 2014, and many others ...

Numerical simulations:

Peregrine 1966, Wei et al. 1995, Soares Frazao and Zech 2002, Lubin et al. 2010, Pan & Lu 2011, Tissier et al. 2011, Simon 2013, Filippini et al. 2018, and many others ...



$$C_\phi + u_2 = C_b$$

$$C_\phi = \left(\frac{g}{k} \tanh(kd_2) \right)^{1/2}$$

conditions de saut pour le ressaut moyen

$$C_b - u_1 = - \left(\frac{gd_2}{2d_1} (d_2 + d_1) \right)^{1/2}$$

$$C_b - u_2 = - \left(\frac{gd_1}{2d_2} (d_2 + d_1) \right)^{1/2}$$

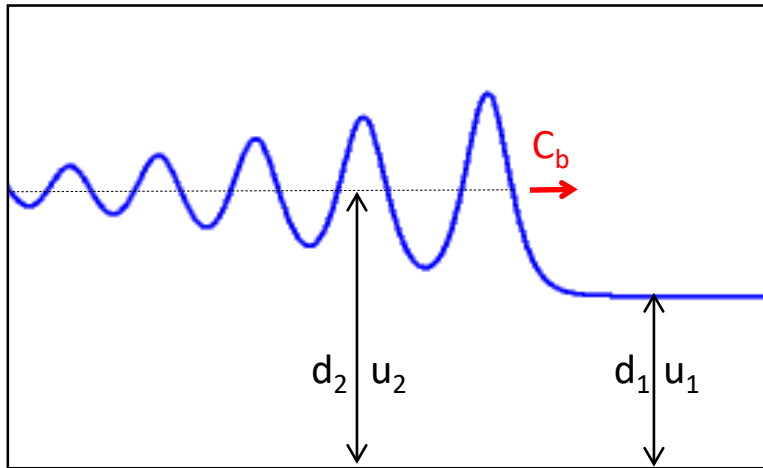
$$\frac{\lambda}{d_1} = f(F_r)$$

$$F_r = \frac{C_b - u_1}{gd_1}$$

$$\frac{\lambda}{d_1} \simeq \frac{\sqrt{2}\pi}{\sqrt{3}} (F_r - 1)^{-1/2}$$

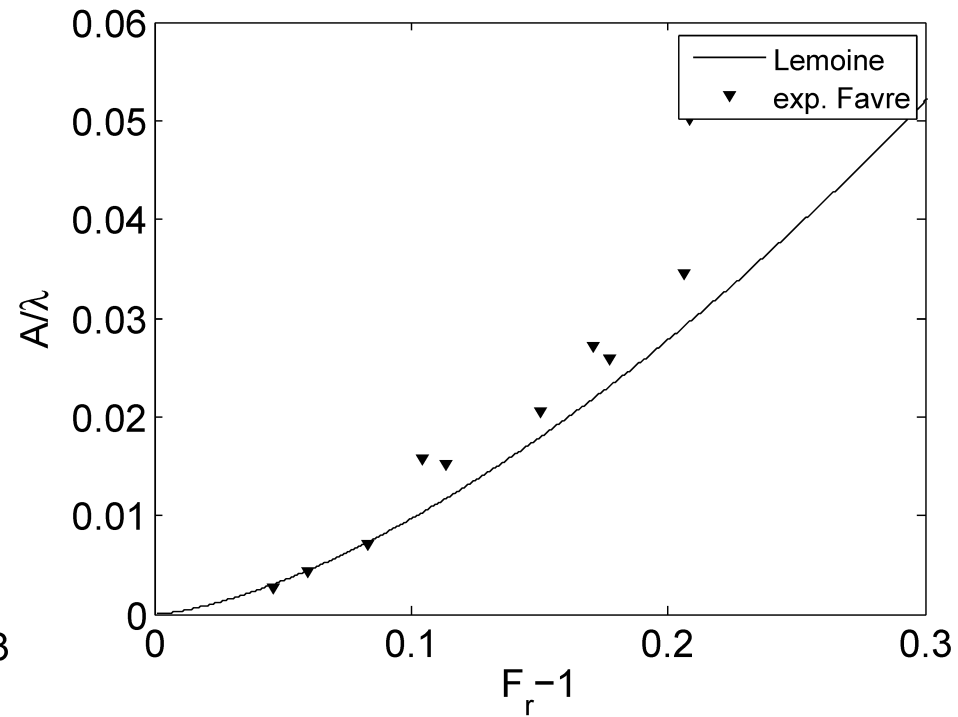
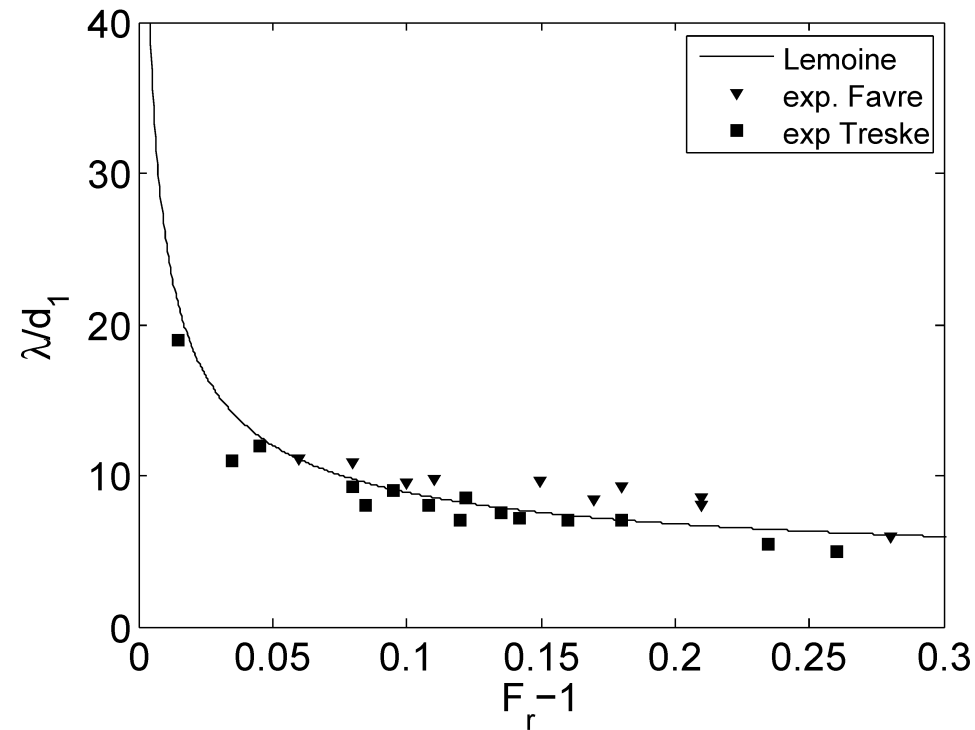
Ondes de Favre

Approche de Lemoine



$$\frac{\lambda}{d_1} \simeq \frac{\sqrt{2}\pi}{\sqrt{3}} (F_r - 1)^{-1/2}$$

$$\frac{A}{\lambda} \simeq \frac{4}{3\sqrt{2}\pi} (F_r - 1)^{3/2}$$



Ondes de Favre : onde 2D → canaux rectangulaires

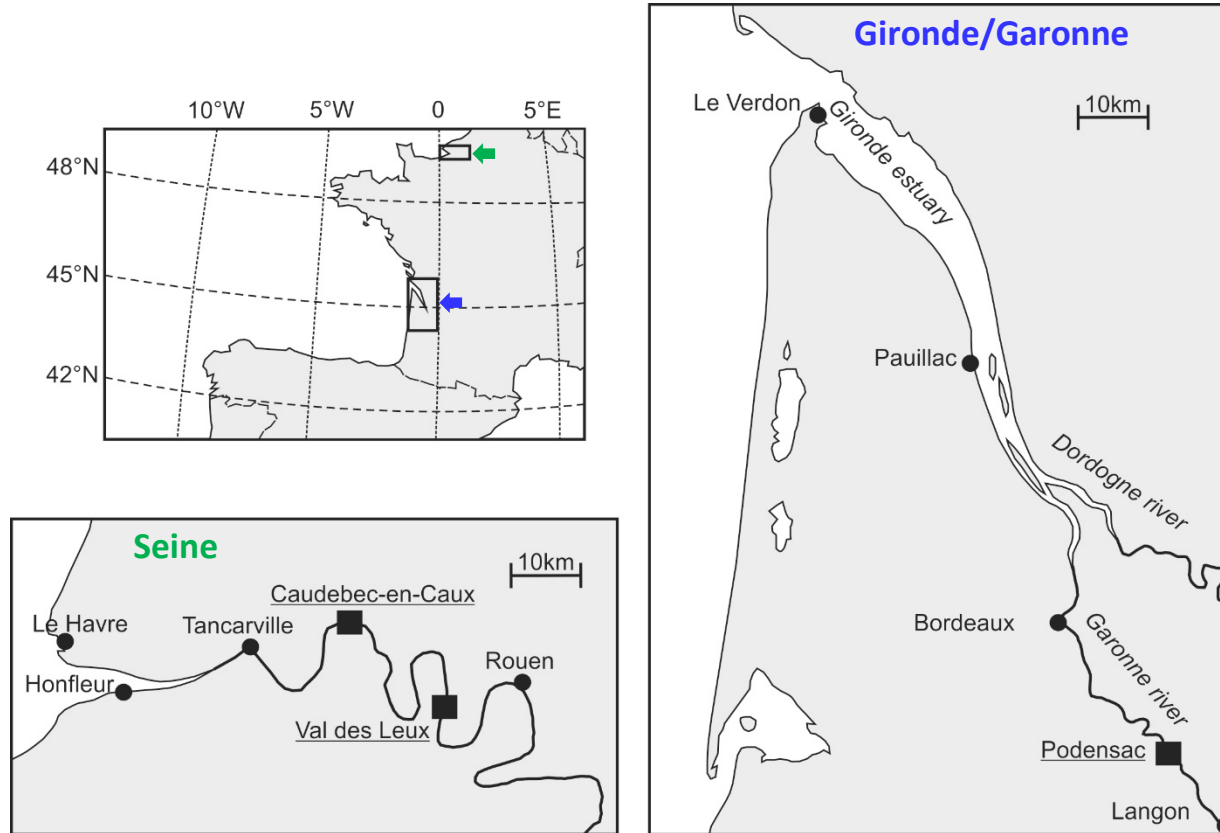
Ressauts de marée



→ influence très grande de la pente des berges

Plan

- I. Introduction
- II. Ondes de Favre
- III. Observations in situ
- IV. Ressaut de marée de faible cambrure
- V. Conclusion and perspectives



- Plus de 200 marées observées sur le système estuarien Gironde/Garonne
→ très large gamme de marnage et débit fluvial
- Mesures complémentaires sur la Seine

Podensac field site (Gironde/Garonne)



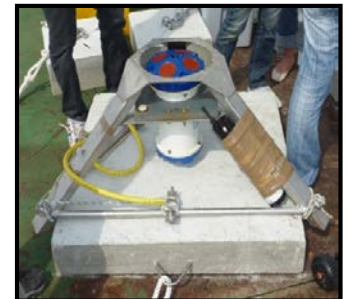
High-frequency measurements

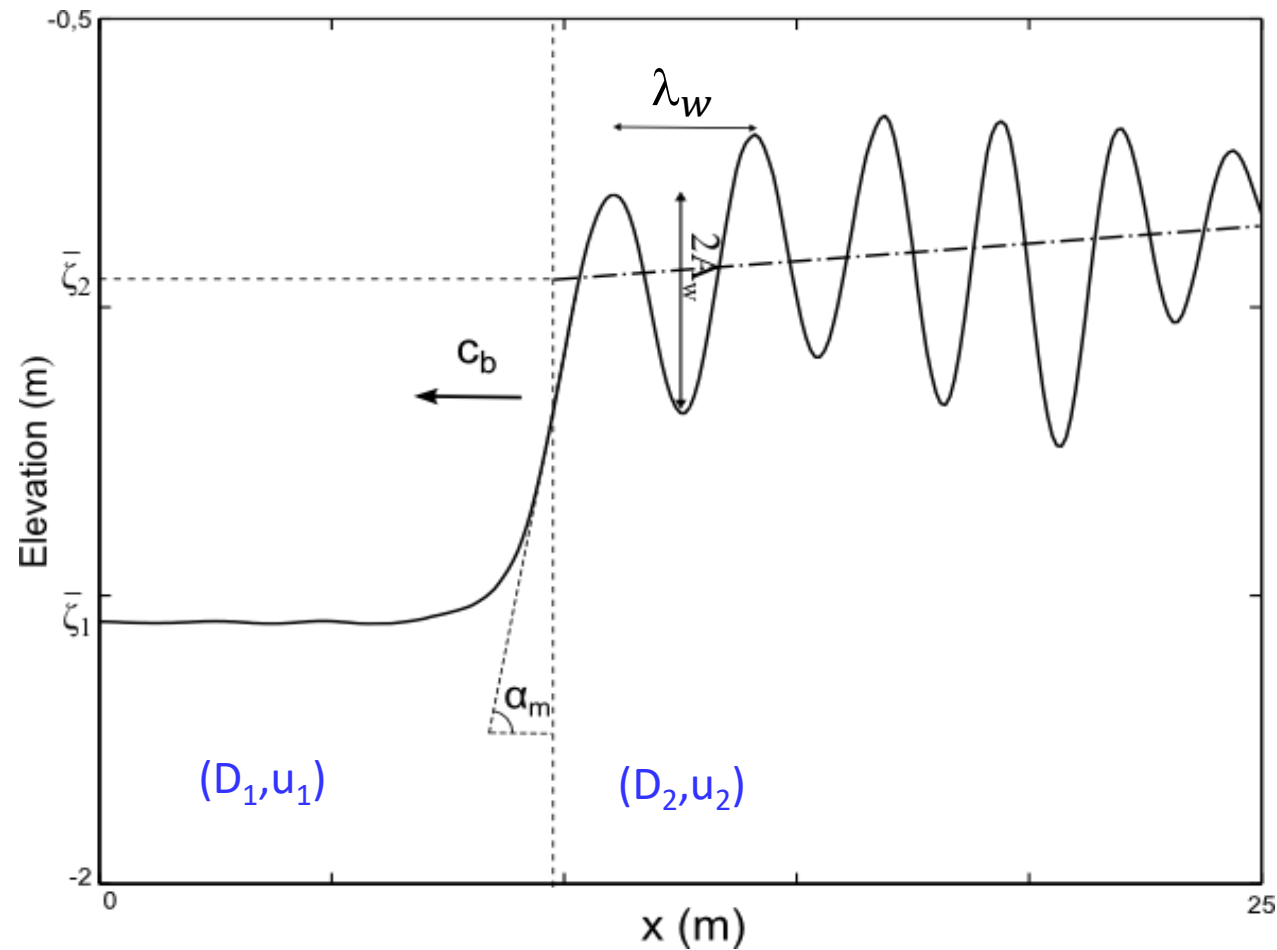


Pressure sensors
(10 Hz)

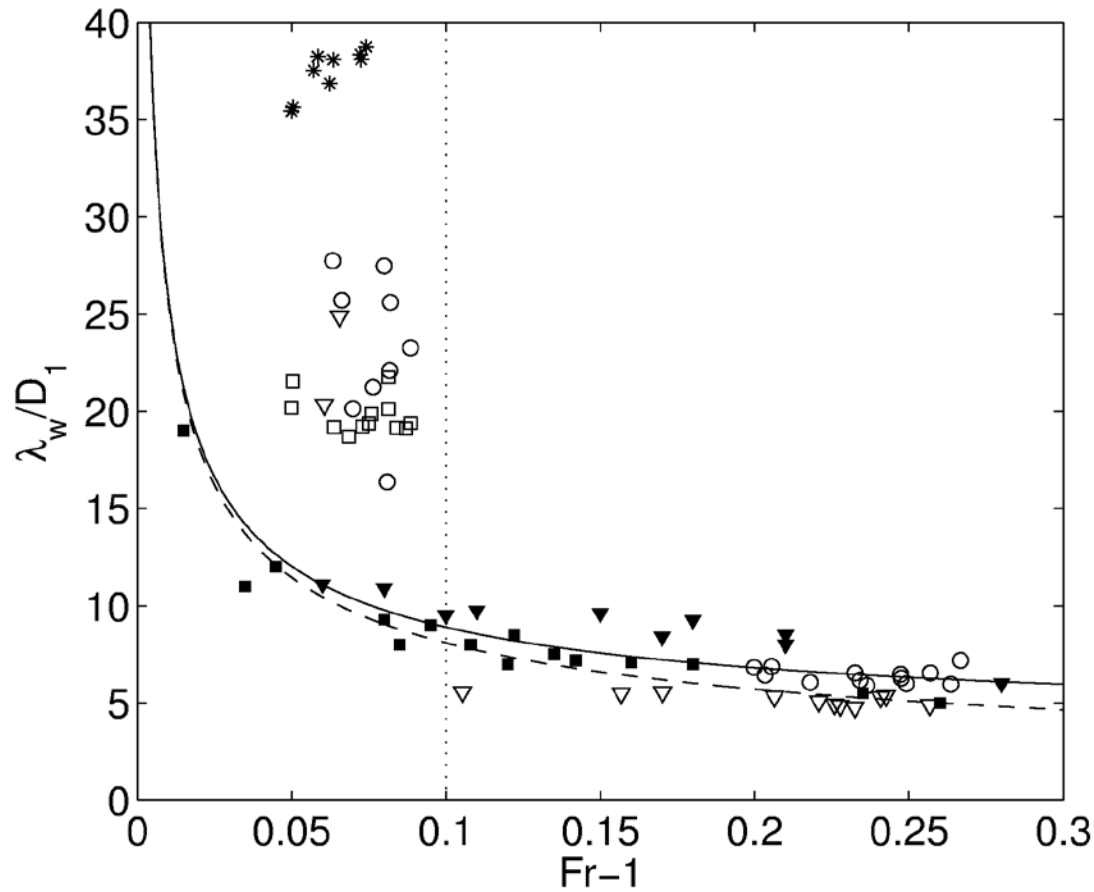


Acoustic Doppler current profilers
(2-8 Hz)

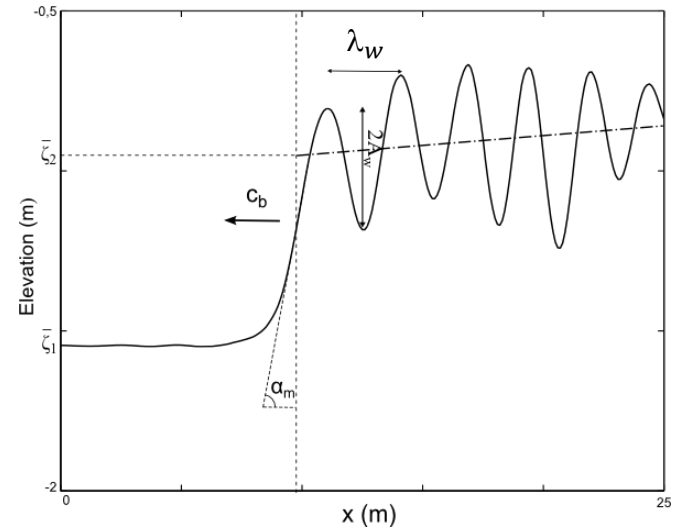




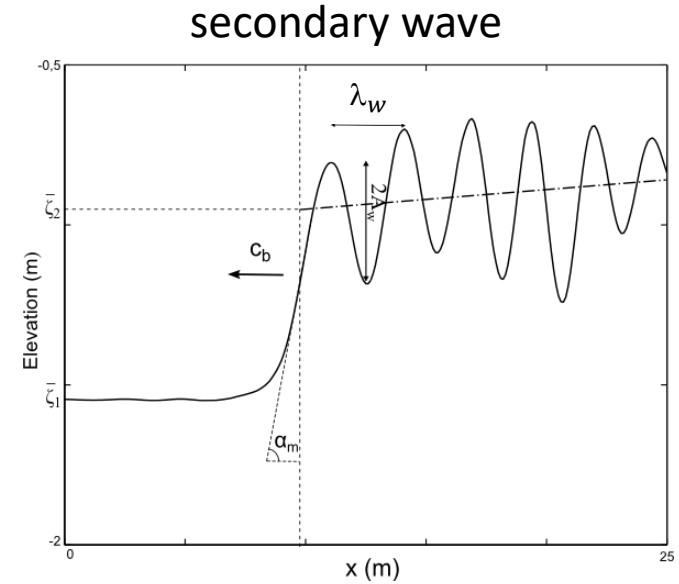
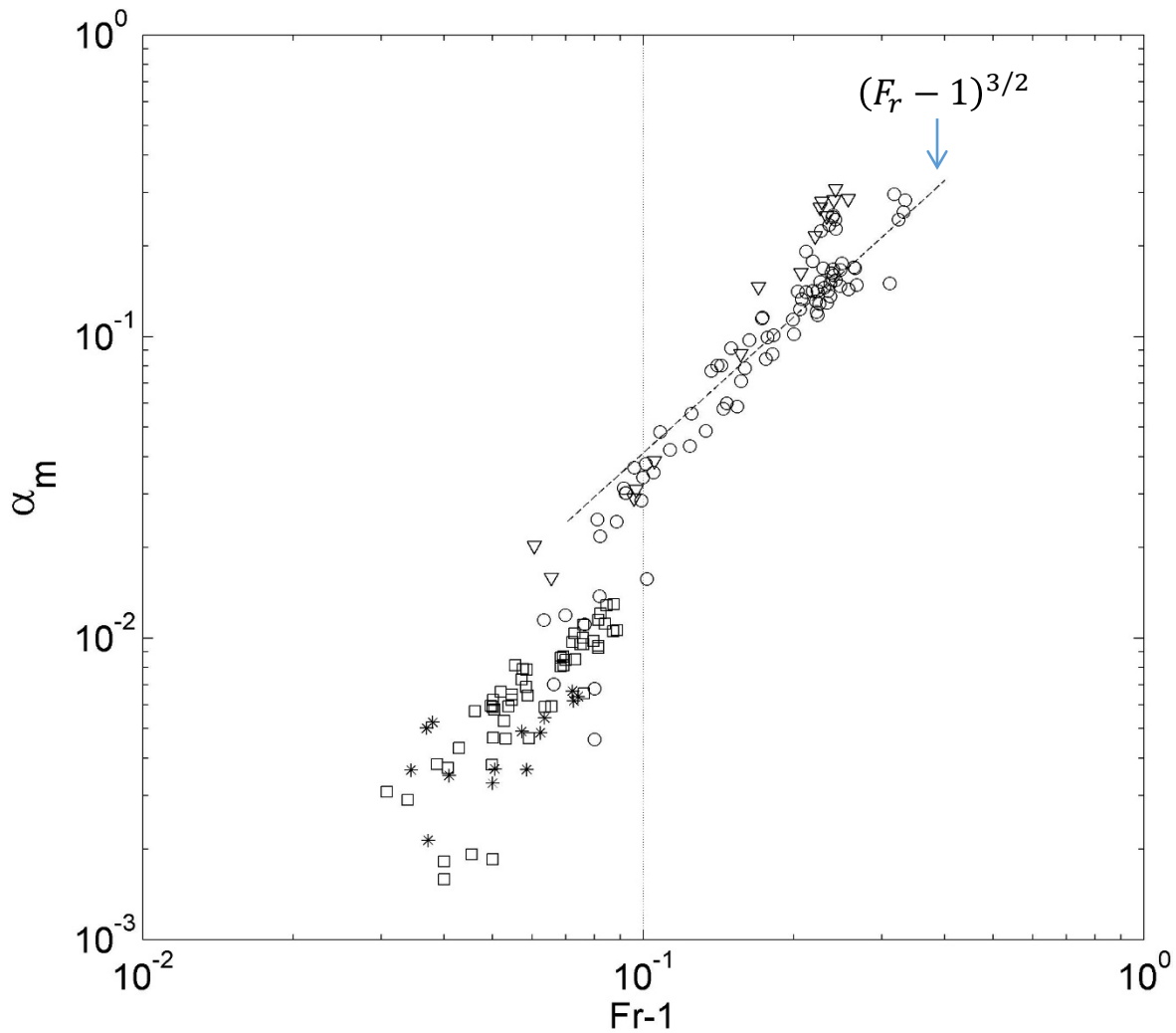
λ_w, A_w, α_m : mesurés dans l'axe de la rivière



Transition at $Fr = Fr_T$ ($Fr_T \approx 1.1$)



$$\frac{\lambda_w}{D_1} = \frac{\pi}{\sqrt{3}} (Fr - 1)^{-1/2}$$

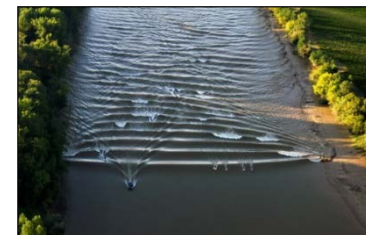


→ Transition at $Fr = Fr_T$ ($Fr_T \approx 1.1$)

-----> <-----

Low steepness secondary wave regime
→ not readily visually observable

high steepness secondary wave regime
→ *mascaret*

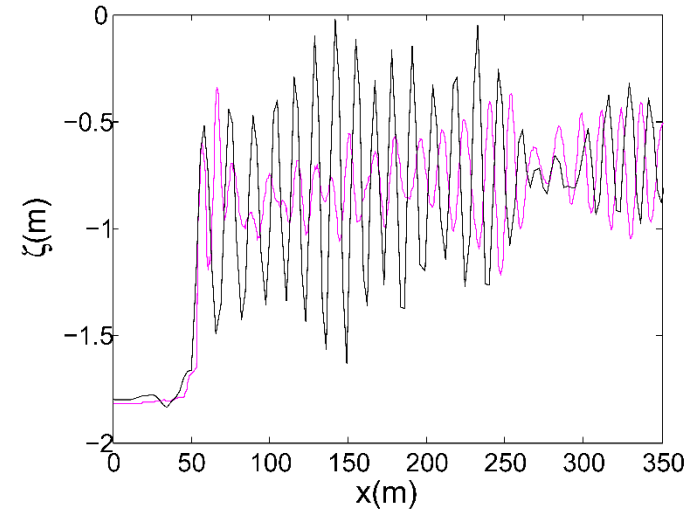


$$\underline{F_B} > \underline{F} > \underline{F_T}$$

high-steepness regime

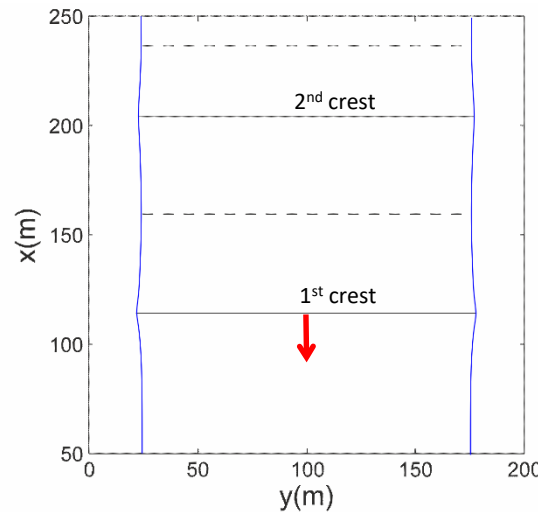


2D phase structure $\phi(x,y)$

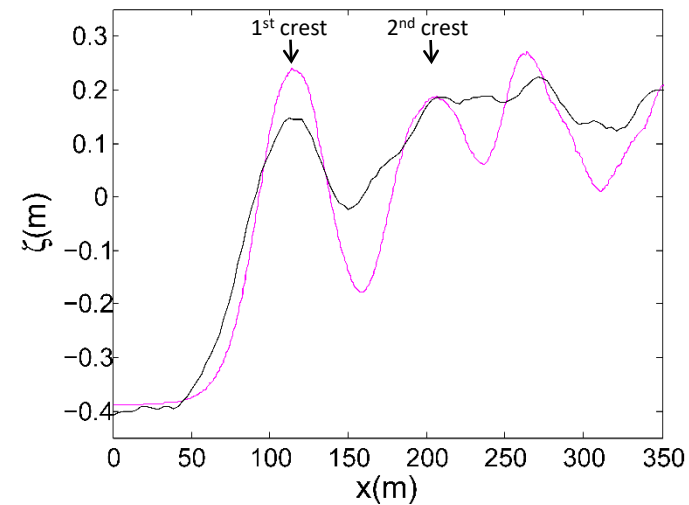


$$\underline{F_T} > \underline{F} > 1$$

low-steepness regime



quasi-1D phase structure $\phi(x)$



Bores on trapezoidal channels Treske (1994)

$F_B > F > F_T$

high-steepness regime

2D phase structure $\phi(x,y)$

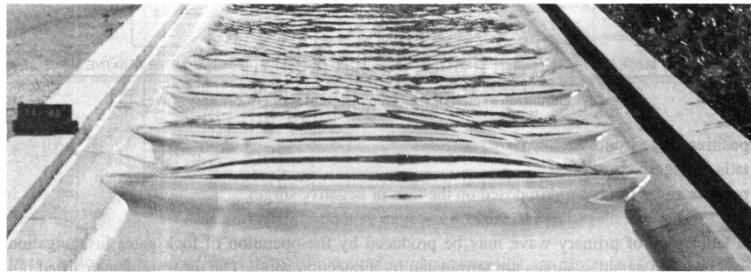


Fig. 11. Undular bore at Froude ~ 1.12.

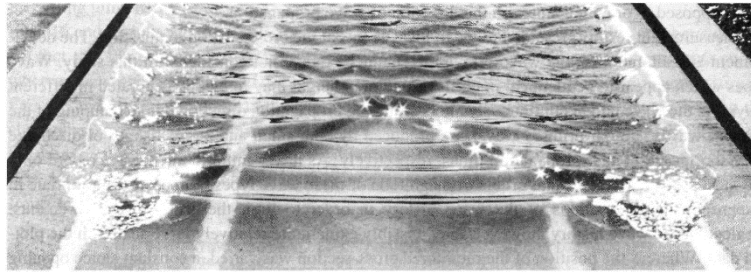


Fig. 12. Undular bore at Froude ~ 1.24.

$F_T > F > 1$

low-steepness regime

1D phase structure $\phi(x)$

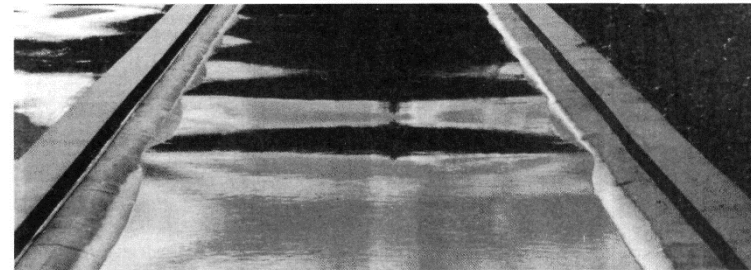


Fig. 9. Undular bore at Froude ~ 1.06.

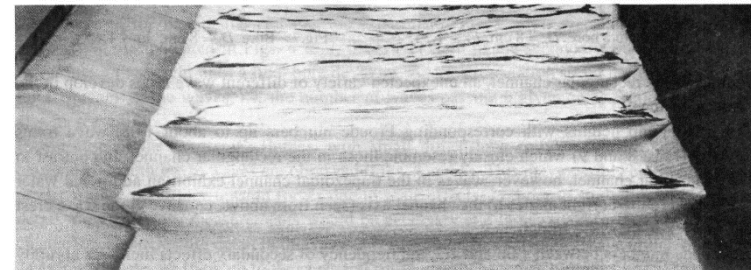
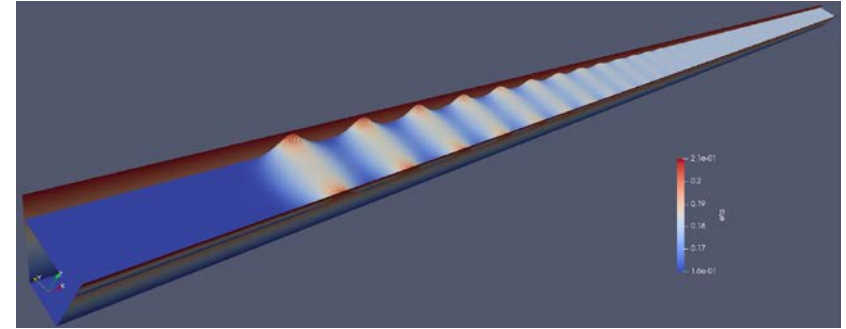
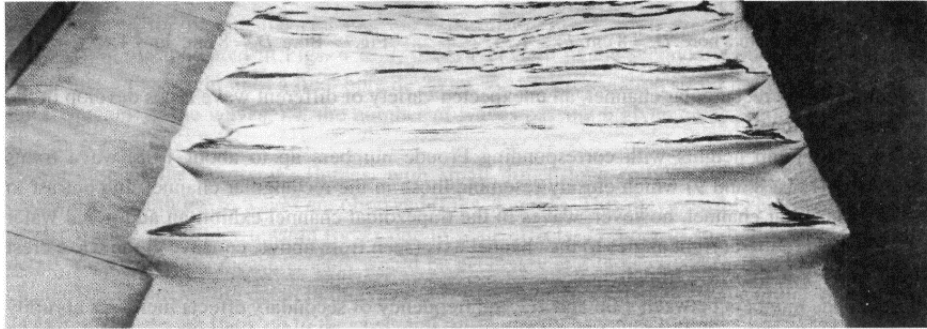


Fig. 10. Undular bore at Froude ~ 1.10.

Plan

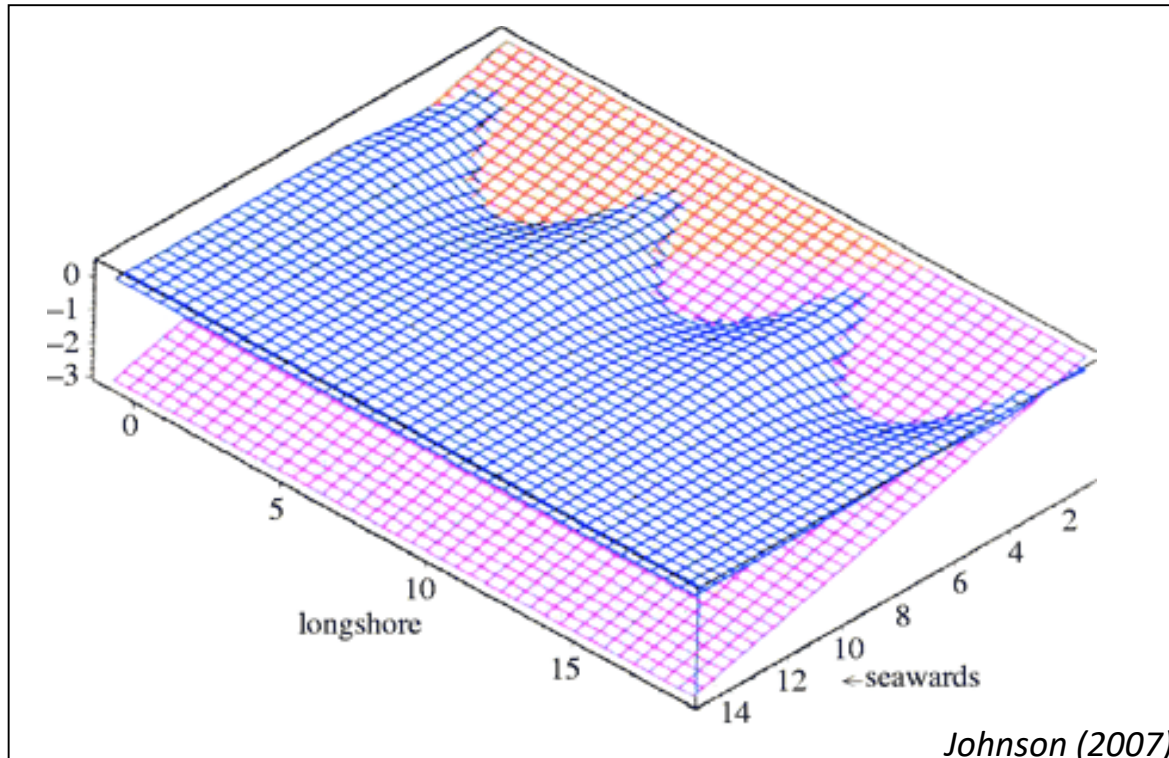
- I. Introduction
- II. Ondes de Favre
- III. Observations in situ
- IV. Ressaut de marée de faible cambrure
- V. Conclusion and perspectives



Chassagne R., Filippini A., Ricchiuto M. and Bonneton P. 2018. Dispersive-like bores in channels with sloping banks. In preparation

analogies avec les ondes de coin (edge waves)?

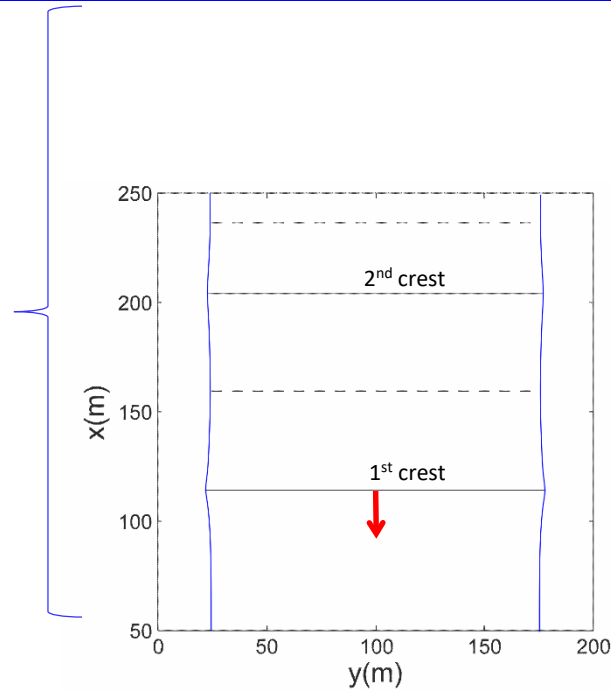
→ ondes longues (infragravitaires, tsunamis, ...) piégées par réfraction



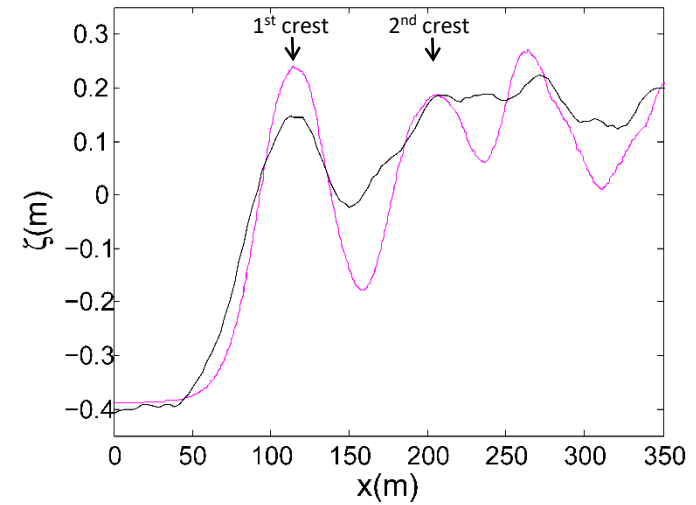
- propagation parallèlement à la plage
- structure de phase 1D
- décroissance de l'amplitude vers le large

- ondes longues décrites par les équations hyperboliques de Saint Venant 2D
- comportement similaire à des ondes dispersives 1D

$\underline{F_T > F > 1}$
 low-steepness regime

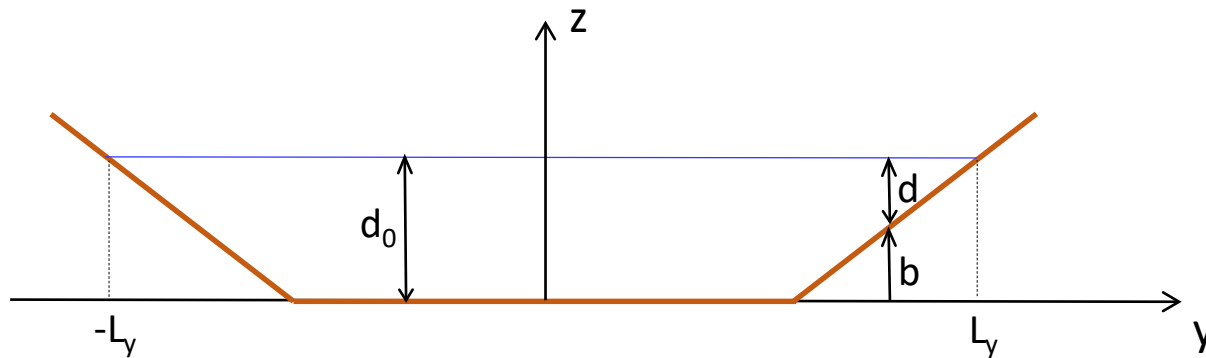


quasi-1D phase structure $\phi(x)$



intégration des équations de SV 2D le long de la section de la rivière

→ équation d'onde 1D pour $\bar{\zeta}(x,t)$



$$d(y) = d_0 - b(y)$$

$$h(x, y, t) = d(y) + \zeta(x, y, t)$$

Equations de Saint Venant linéarisées 2D

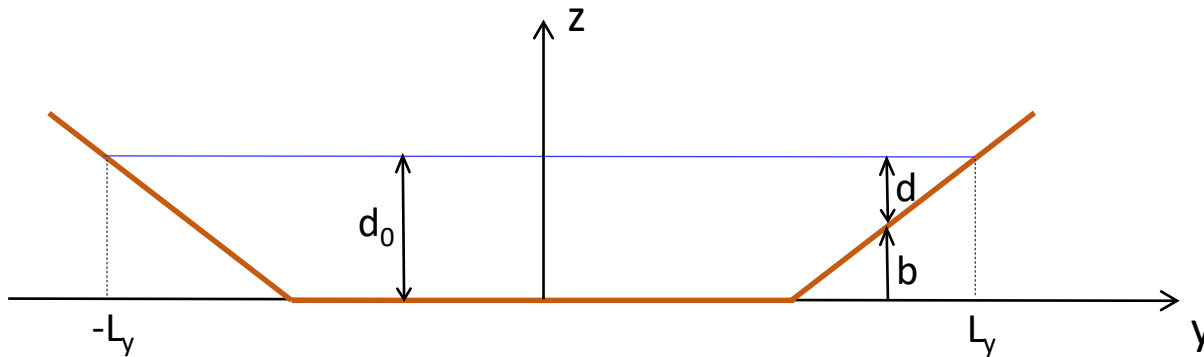
$$\frac{\partial \zeta}{\partial t} + d \frac{\partial u}{\partial x} + \frac{\partial dv}{\partial y} = 0$$

$$\frac{\partial u}{\partial t} + g \frac{\partial \zeta}{\partial x} = 0$$

$$\frac{\partial v}{\partial t} + g \frac{\partial \zeta}{\partial y} = 0$$

$$\frac{\partial^2 \zeta}{\partial t^2} - C^2 \Delta \zeta - g \frac{\partial d}{\partial y} \frac{\partial \zeta}{\partial y} = 0,$$

$$\text{with } C = \sqrt{gd}.$$



$$d(y) = d_0 - b(y)$$

$$h(x,y,t) = d(y) + \zeta(x,y,t)$$

$$\overline{(\cdot)} = \frac{1}{2L_y} \int_{-L_y}^{L_y} (\cdot) dy$$

$$\frac{\partial^2 \bar{\zeta}}{\partial t^2} - \overline{gd} \frac{\partial^2 \zeta}{\partial x^2} = 0,$$

$$\frac{\partial^2 \bar{\zeta}}{\partial t^2} - C_m^2 \frac{\partial^2 \bar{\zeta}}{\partial x^2} - \overline{g(d - \bar{d})} \frac{\partial^2 \zeta}{\partial x^2} = 0,$$

$$\text{with } C_m = \sqrt{g\bar{d}}.$$

adimensionnement des équations

$$x' = \frac{x}{L_x}, \quad y' = \frac{y}{L_y}, \quad d' = \frac{d}{\bar{d}}, \quad \zeta' = \frac{\zeta}{A}$$

$$t' = \frac{t}{L_x/C_m}, \quad u' = \frac{u}{AC_m/\bar{d}}, \quad v' = \frac{v}{AC_m/\bar{d}}$$

$$\delta \frac{\partial \zeta}{\partial t} + \delta d \frac{\partial u}{\partial x} + \frac{\partial v}{\partial y} = 0$$

$$\frac{\partial u}{\partial t} + \frac{\partial \zeta}{\partial x} = 0$$

$$\delta \frac{\partial v}{\partial t} + \frac{\partial \zeta}{\partial y} = 0$$

$$\frac{\partial^2 \bar{\zeta}}{\partial t^2} - d \frac{\partial^2 \zeta}{\partial x^2} = 0$$

$$\delta = \frac{L_y}{L_x} \ll 1$$

$$\zeta = \sum_{i \geq 0} \delta^i \zeta_i$$

Ordre O(1)

$$\begin{aligned} \frac{\partial v_0}{\partial y} &= 0 \\ \frac{\partial u_0}{\partial t} + \frac{\partial \zeta_0}{\partial x} &= 0 \\ \frac{\partial \zeta_0}{\partial y} &= 0 \end{aligned}$$



$$\begin{aligned} v_0 &= 0 \\ u_0 &= \bar{u}_0 \\ \zeta_0 &= \bar{\zeta}_0 \end{aligned}$$

$$\frac{\partial^2 \bar{\zeta}_0}{\partial t^2} - \frac{\partial^2 \bar{\zeta}_0}{\partial x^2} = 0$$

Ordre $O(\delta)$

$$\begin{array}{l}
 \frac{\partial dv_1}{\partial y} = -\frac{\partial \zeta_0}{\partial t} - d \frac{\partial u_0}{\partial x} \\
 \frac{\partial u_1}{\partial t} + \frac{\partial \zeta_1}{\partial x} = 0 \\
 \frac{\partial \zeta_1}{\partial y} = 0
 \end{array}
 \rightarrow
 \begin{array}{l}
 v_1 = -\frac{y+1}{d} \frac{\partial \bar{\zeta}_0}{\partial t} - \frac{D}{d} \frac{\partial \bar{u}_0}{\partial x} \\
 u_1 = \bar{u}_1 \\
 \zeta_1 = \bar{\zeta}_1
 \end{array}$$

$$D = \int_{-1}^y d(s) ds$$

$$\frac{\partial^2 \bar{\zeta}_1}{\partial t^2} - \frac{\partial^2 \bar{\zeta}_1}{\partial x^2} = 0$$

Ordre $O(\delta^2)$

$$\begin{aligned}\frac{\partial v_2}{\partial y} &= -\frac{\partial \zeta_1}{\partial t} - d \frac{\partial u_1}{\partial x} \\ \frac{\partial u_2}{\partial t} + \frac{\partial \zeta_2}{\partial x} &= 0 \\ \frac{\partial \zeta_2}{\partial y} &= -\frac{\partial v_1}{\partial t}\end{aligned}$$

→

$$\zeta_2 = \bar{\zeta}_2 + (K(y) - \bar{K}) \frac{\partial^2 \bar{\zeta}_0}{\partial x^2}$$

$$K = \int_{-1}^y \frac{(y+1-D)}{d} ds$$

Ordre $O(\delta^2)$

$$\begin{array}{r}
 \frac{\partial dv_2}{\partial y} = -\frac{\partial \zeta_1}{\partial t} - d \frac{\partial u_1}{\partial x} \\
 \frac{\partial u_2}{\partial t} + \frac{\partial \zeta_2}{\partial x} = 0 \\
 \frac{\partial \zeta_2}{\partial y} = -\frac{\partial v_1}{\partial t}
 \end{array}
 \rightarrow
 \zeta_2 = \bar{\zeta}_2 + (K(y) - \bar{K}) \frac{\partial^2 \bar{\zeta}_0}{\partial x^2}$$

$$K = \int_{-1}^y \frac{(y+1-D)}{d} ds$$

$$\zeta = \zeta_0 + \delta \zeta_1 + \delta^2 \zeta_2 = \bar{\zeta} + \delta^2 (K(y) - \bar{K}) \frac{\partial^2 \bar{\zeta}}{\partial x^2} + O(\delta^3)$$

$$\frac{\partial^2 \bar{\zeta}}{\partial t^2} - \frac{\partial^2 \bar{\zeta}}{\partial x^2} - \delta^2 \chi \frac{\partial^4 \bar{\zeta}}{\partial x^4} = 0$$

$$\chi = \overline{d(K(y) - \bar{K})}$$

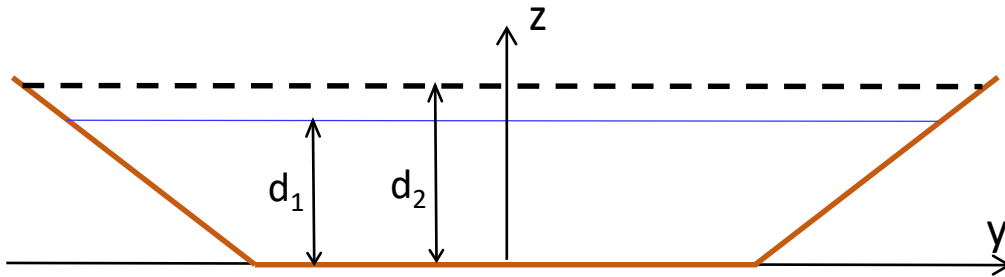
$$\frac{\partial^2 \bar{\zeta}}{\partial t^2} - \frac{\partial^2 \bar{\zeta}}{\partial x^2} - \delta^2 \chi \frac{\partial^4 \bar{\zeta}}{\partial x^4} = 0$$

$$\bar{\zeta} = A \exp(i(kx - \omega t))$$

$$C_\phi^2 = \frac{\omega^2}{k^2} = 1 - \delta^2 \chi k^2$$

$$C_\phi = C_m (1 - \chi k^2)^{1/2}$$

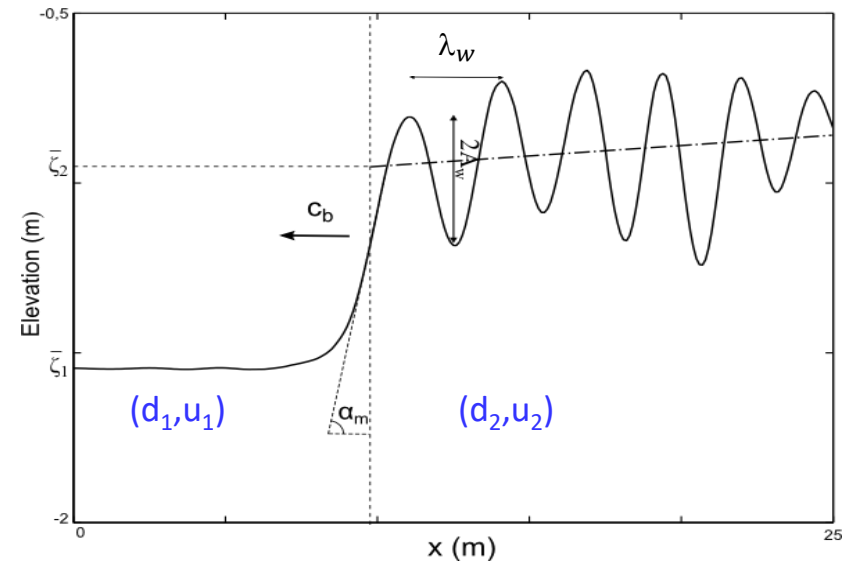
$$C_m = \sqrt{g\bar{d}}$$



$$C_\phi + u_2 = C_b$$

$$C_\phi = C_m (1 - \chi k^2)^{1/2}$$

$$\lambda = 2\pi\chi^{1/2} \left(1 - \frac{(C_b - u_2)^2}{g\bar{d}_2} \right)^{1/2}$$



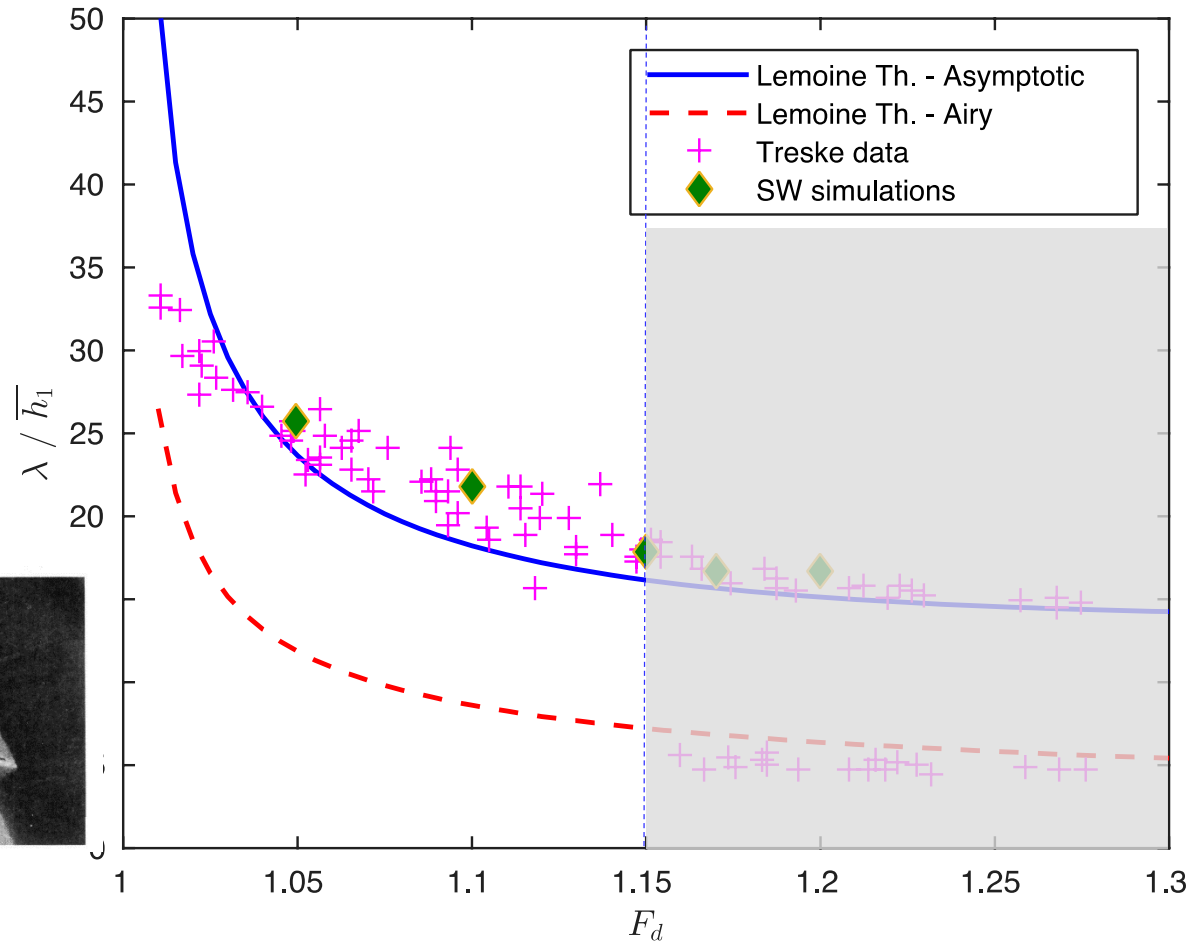
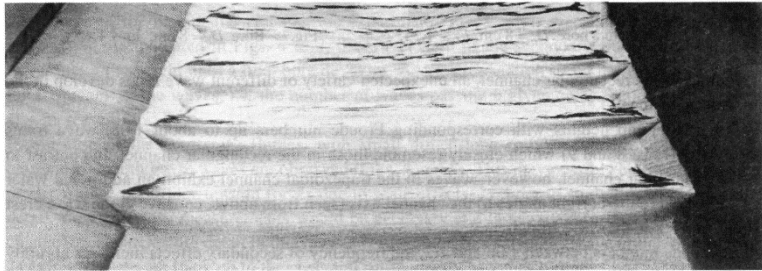
Conditions de saut pour le ressaut moyen

$$C_b - u_1 = \sqrt{g \frac{A_2}{A_1} \frac{\mathcal{K}_2 - \mathcal{K}_1}{A_2 - A_1}}$$

$$C_b - u_2 = \sqrt{g \frac{A_1}{A_2} \frac{\mathcal{K}_2 - \mathcal{K}_1}{A_2 - A_1}}$$

$$\mathcal{K} = \int A dh$$

Treske (1994)

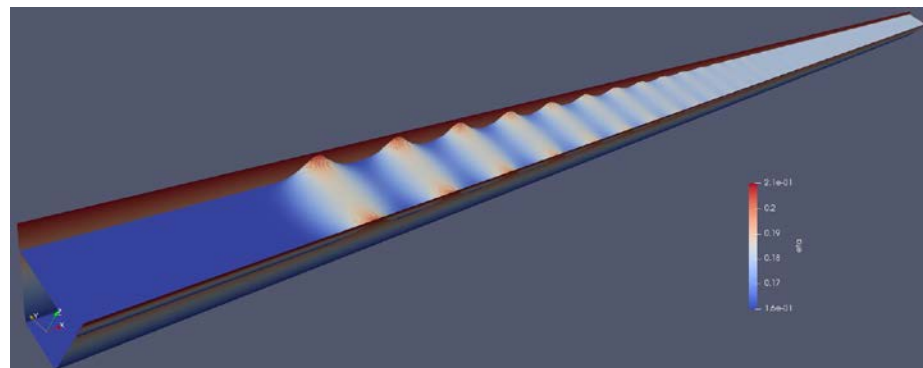
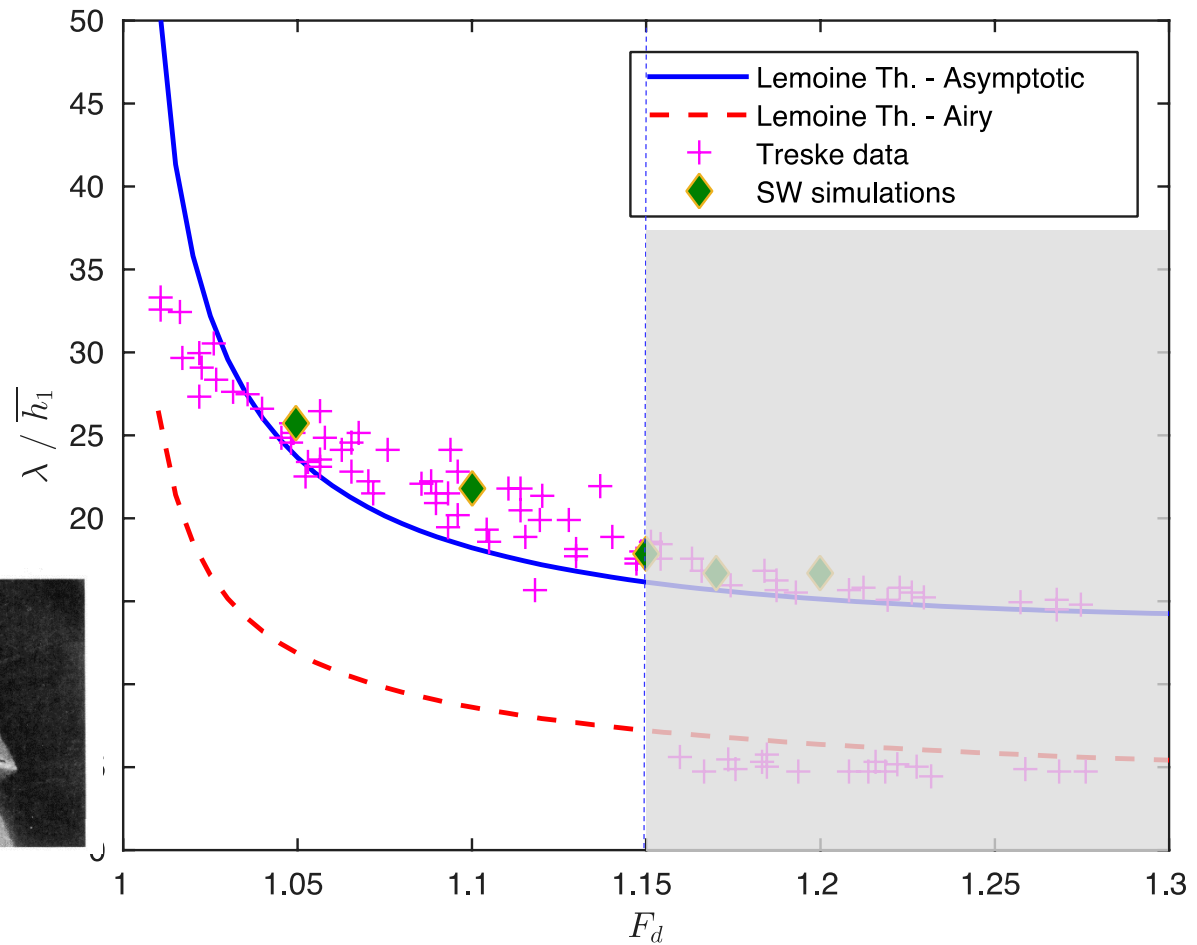
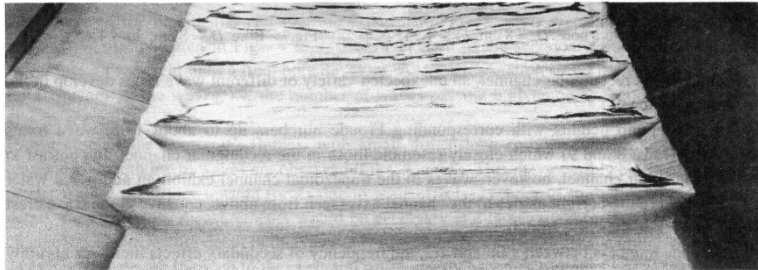


Transition at $Fr = F_T$



Low steepness
secondary wave regime

Treske (1994)



Conclusion et perspectives

□ Identification d'un nouveau régime d'écoulement

pour les ressauts de marée ondulants

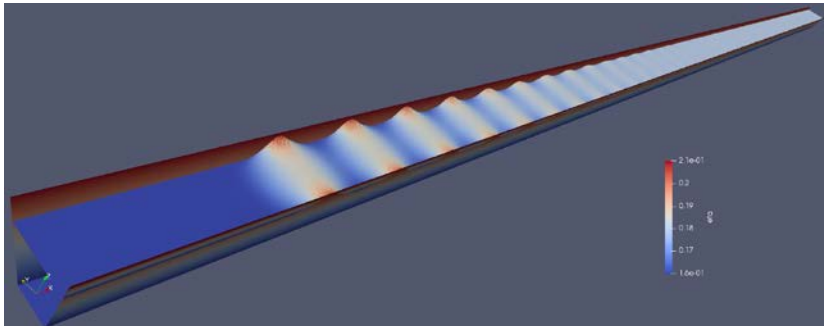
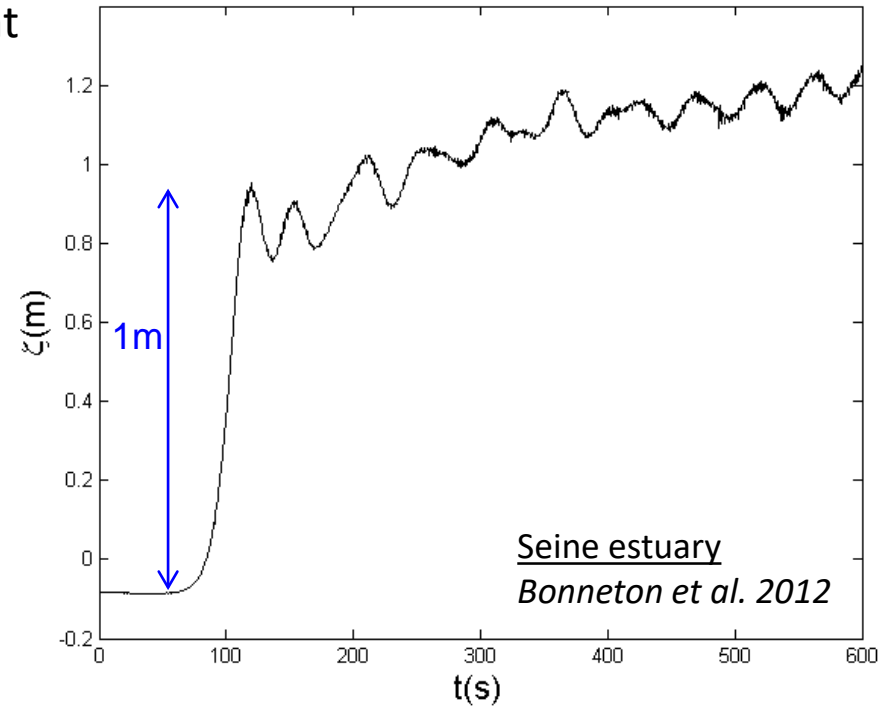
→ RM à faible cambrure

□ Dynamique contrôlée par la réfraction

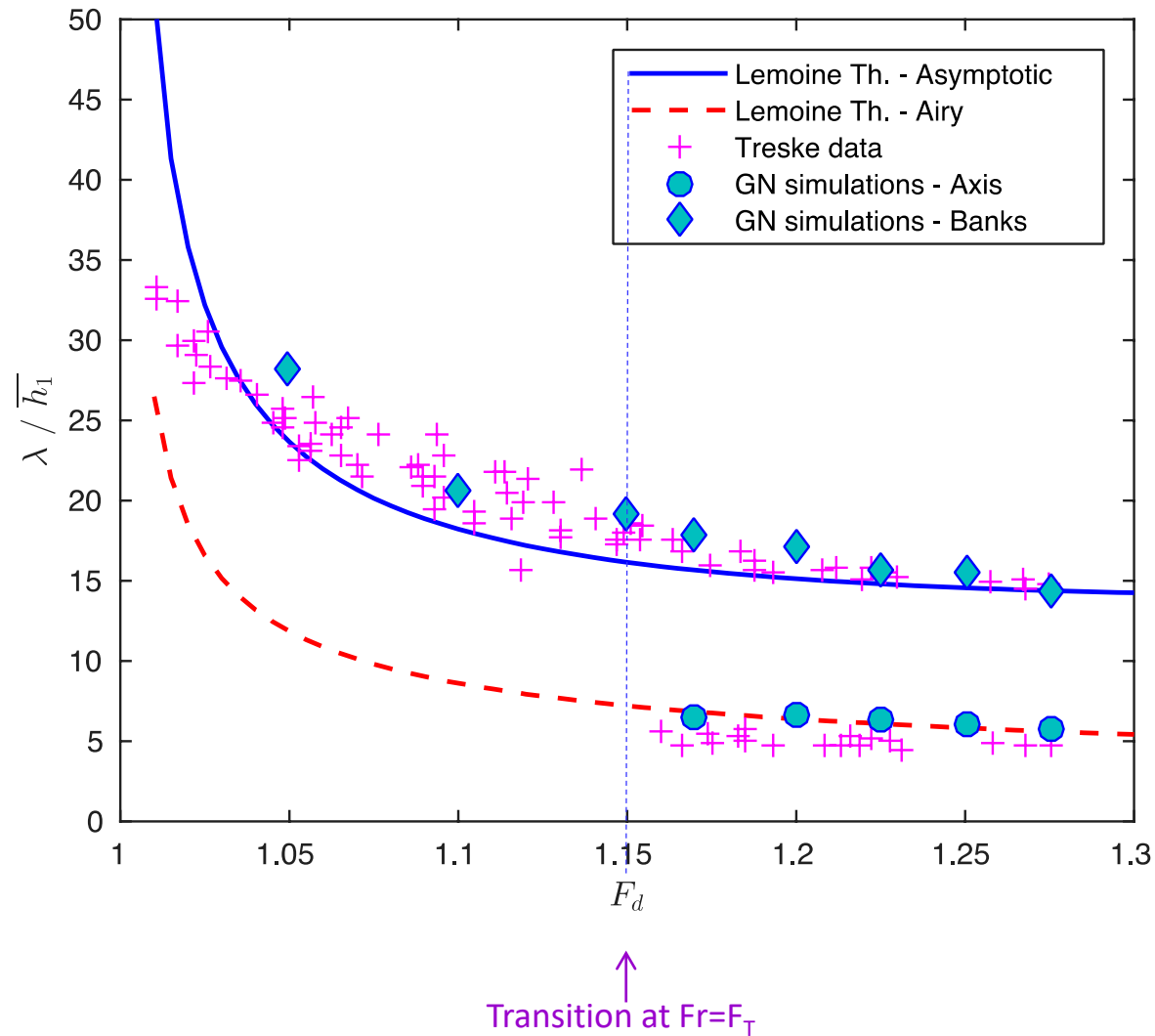
sur les berges

→ équation d'onde 1D de nature dispersive

$$\frac{\partial^2 \bar{\zeta}}{\partial t^2} - \frac{\partial^2 \bar{\zeta}}{\partial x^2} - \delta^2 \chi \frac{\partial^4 \bar{\zeta}}{\partial x^4} = 0$$



Conclusion et perspectives



Simulations numériques
Serre-Green Naghdi
Chassagne et al. 2018

➤ Quels mécanismes contrôlent la transition à $F = F_T$?

Merci de votre attention

